

Optical observations of NEA 3200 Phaethon (1983 TB) during the 2017 apparition[★]

M.-J. Kim¹, H.-J. Lee^{1,2}, S.-M. Lee^{1,2}, D.-H. Kim^{1,2}, F. Yoshida³, P. Bartczak⁴, G. Dudziński⁴, J. Park¹, Y.-J. Choi^{1,5}, H.-K. Moon¹, H.-S. Yim¹, J. Choi^{1,5}, E.-J. Choi¹, J.-N. Yoon⁶, A. Serebryanskiy⁷, M. Krugov⁷, I. Reva⁷, K. E. Ergashev⁸, O. Burkhonov⁸, S. A. Ehgamberdiev⁸, Y. Turayev⁸, Z.-Y. Lin⁹, T. Arai³, K. Ohtsuka¹⁰, T. Ito¹¹, S. Urakawa¹², and M. Ishiguro¹³

¹ Korea Astronomy and Space Science Institute, 776, Daedeokdae-ro, Yuseong-gu, Daejeon 34055, Korea

e-mail: skarma@kasi.re.kr

² Chungbuk National University, 1 Chungdae-ro, Seowon-gu, Cheongju, Chungbuk 28644, Korea

³ Planetary Exploration Research Center, Chiba Institute of Technology, 2-17-1 Tsudanuma, Narashino, Chiba 275-0016, Japan

⁴ Astronomical Observatory Institute, Faculty of Physics, Adam Mickiewicz University, Słoneczna 36, 60-286 Poznań, Poland

⁵ University of Science and Technology, 217, Gajeong-ro, Yuseong-gu, Daejeon 34113, Korea

⁶ Chungbuk National University Observatory, 802-3 Euntan-ri, Jincheon-gun, Chungcheongbuk-do, Korea

⁷ Fesenkov Astrophysical Institute, Observatory 23, 050020 Almaty, Kazakhstan

⁸ Ulugh Beg Astronomical Institute of the Uzbekistan Academy of Sciences, 33 Astronomicheskaya str., Tashkent, 100052, Uzbekistan

⁹ Institute of Astronomy, National Central University, No. 300, Zhongda Rd., Zhongli Dist., Taoyuan City 32001, Taiwan

¹⁰ Tokyo Meteor Network, Daisawa 1-27-5, Setagaya-ku, Tokyo 155-0032, Japan

¹¹ National Astronomical Observatory of Japan, Osawa 2-21-1, Mitaka, Tokyo 181-8588, Japan

¹² Japan Spaceguard Association, Bisei Spaceguard Center, 1716-3 Okura, Bisei-cho, Ibara, Okayama 714-1411, Japan

¹³ Seoul National University, 1 Gwanak-ro, Gwanak-gu, Seoul 08826, Korea

Received June 08, 2018; accepted Aug 30, 2018

[★] Photometric data will be available in electronic form at the CDS via anonymous ftp to cdsarc.u-strasbg.fr (130.79.128.5) or via <http://cdsarc.u-strasbg.fr/viz-bin/qcat?J/A+A/volume/page>

ABSTRACT

Context. The near-Earth asteroid 3200 Phaethon (1983 TB) is an attractive object not only from a scientific viewpoint but also because of JAXA's DESTINY⁺ target. The rotational lightcurve and spin properties were investigated based on the data obtained in the ground-based observation campaign of Phaethon.

Aims. We aim to refine the lightcurves and shape model of Phaethon using all available lightcurve datasets obtained via optical observation, as well as our time-series observation data from the 2017 apparition.

Methods. Using eight 1–2-m telescopes and an optical imager, we acquired the optical lightcurves and derived the spin parameters of Phaethon. We applied the lightcurve inversion method and SAGE (Shaping Asteroids with Genetic Evolution) algorithm to deduce the convex and non-convex shape model and pole orientations.

Results. We analysed the optical lightcurve of Phaethon and derived a synodic and a sidereal rotational periods of 3.6039 h, with an axis ratio of $a/b = 1.07$. The ecliptic longitude (λ_p) and latitude (β_p) of the pole orientation were determined as (308, -52) and (322, -40) via two independent methods. A non-convex model from the SAGE method, which exhibits a concavity feature, is also presented.

Key words. Minor planets, asteroids: individual: 3200 Phaethon (1983 TB)

1. Introduction

The near-Earth asteroid (NEA) (3200) Phaethon (1983 TB) (hereinafter referred to as Phaethon) is the target of the DESTINY⁺ mission, which is an Epsilon-class programme, and is currently under Phase-A study by JAXA (Japan Aerospace Exploration Agency)/ISAS (Institute of Space and Astronautical Science). Phaethon is classified as a member of the Apollo asteroidal group with a semi-major axis greater than that of the Earth. In addition, it is called as Mercury-crosser asteroid with the small perihelion distance of only 0.14 AU. It is also categorised as a potentially hazardous asteroid; the Earth minimum orbit intersection distance is 0.01945 AU. The spectral type of Phaethon is known as B-type (Green et al. 1985; Binzel et al. 2001, 2004; Bus & Binzel 2002), which is a sub-group of C-complex that is attributed to primitive volatile-rich remnants from early solar system. The asteroid (24) Themis - a typical B-type asteroid - was recently discovered to have H₂O ice and organic matter on its surface (Rivkin & Emery 2010; Campins et al. 2010). Phaethon is thus one of the most remarkable NEAs, not only because of its spectral type but also because of its extraordinary connection with the Geminids meteor shower that occurs every mid-December (Gustafson 1989; Williams & Wu 1993; Jenniskens 2006, and references therein).

For this reason, various investigations of the physical properties of Phaethon have been conducted. Regarding the rotational properties, the most recent results of lightcurve observations in-

** Demonstration and Experiment of Space Technology for INterplanetary voYage, Phaethon fLyby and dUSt science

Table 1. Observatory and instrument details.

Telescope ^a	λ^b	ϕ^b	Altitude [m]	Instrument ^c [CCD]	Pixel scale [''pix ⁻¹]	Observer ^d
SLT 0.4 m	120:52:25	+23:28:07	2,879.0	e2v CCD42-40	0.79	ZYL
OWL 0.5 m	249:12:38	+32:26:32	2,769.5	FLI 16803	0.98	JC, EJC
SOAO 0.6m	128:27:27	+36:56:04	1,354.4	FLI 16803	0.45	TSJ, GYH
CBNUO 0.6 m	127:28:31	+36:46:53	87.0	STX-16803	1.05	SML, JNY
MAO 0.6 m	66:53:44	+38:40:24	2,578.2	FLI IMG1001E	0.68	EK, OB, SAE, YT
TShAO 1.0 m	76:58:18	+43:03:26	2,723.5	Apogee Alta F16M	0.56	AS, MK, IR
LOAO 1.0 m	249:12:41	+32:26:32	2,776.0	e2v 4K CCD	0.80	FY, JHY, IKB
BOAO 1.8 m	128:58:36	+36:09:53	1,143.0	e2v 4K CCD	0.43	MJK, JP

Notes. ^(a) Abbreviations: SLT = Lulin Super Light Telescope, OWL = Optical Wide-field patrol, SOAO = Sobaeksan Optical Astronomy Observatory, CBNUO = ChungBuk National University Observatory, MAO = Maidanak Astronomical Observatory, TShAO = Tian Shan Astronomical Observatory, LOAO = Lemonsan Optical Astronomy Observatory, BOAO = Bohyunsan Optical Astronomy Observatory ^(b) Eastern longitude and geocentric latitude of each observatory ^(c) FLI 16803 in SOAO, e2v 4K CCD and SI 4K CCD were configured with 2×2 binning ^(d) Observer: ZYL = Zhong-Yi Lin, JC = Jin Choi, EJC = Eun-Jung Choi, TSJ = Taek-Soo Jung, GYH = Gi-Young Han, SML = Sang-Min Lee, JNY = Joh-Na Yoon, EK = Ergashev Kamoliddin, OB = Otobek Burkhonov, SAE = Shuhrat A. Ehgamberdiev, YT = Yunus Turayev, AS = Alexander Serebryanskiy, MK = Maxim Krugov, IR = Inna Reva, FY = Fumi Yoshida, JHY = Jae-Hyuk Yoon, IKB = In-Kyung Baek, MJK = Myung-Jin Kim, JP = Jintae Park

dicates that Phaethon has a rotational period of 3.604 h (Wisniewski et al. 1997; Pravec et al. 1998; Krugly et al. 2002; Ansdell et al. 2014; Warner 2015; Schmidt 2018). On the basis of the lightcurve analysis, Phaethon is regarded as having a nearly spherical shape with a small lightcurve amplitude of 0.1 – 0.2. Ansdell et al. (2014) derived $\lambda = 85^\circ \pm 13^\circ$ and $\beta = -20^\circ \pm 10^\circ$, while Hanuš et al. (2016) obtained a convex shape model of Phaethon and the pole axis of $\lambda = 319^\circ \pm 5^\circ$ and $\beta = -39^\circ \pm 5^\circ$ according to previous and newly obtained lightcurves, where λ and β are the ecliptic longitude and latitude of the pole orientation, respectively.

The observation window for Phaethon at the end of 2017 was a good opportunity to acquire high-quality dense photometric data, as the asteroid passed by the Earth at a lunar distance (LD) of only 27 LD on 16 December 2017, which was the closest approach in 40 years. We performed a photometric observation campaign for Phaethon between the Asian and American continents during the 2017 apparition to investigate its rotational properties and refine the pole solution. In this paper, we outline our optical observations, data reduction, and analysis. We derived the rotational period and peak-to-peak variation from the lightcurve. Furthermore, we deduced the pole orientation and shape model with not only a convex model based on the lightcurve-inversion method (Kaasalainen & Torppa 2001; Kaasalainen et al. 2001) but also a non-convex model using the SAGE (Shaping Asteroids with Genetic Evolution) algorithm (Bartczak & Dudziński 2018).

2. Observations

Photometric observations of Phaethon were conducted for a total of 22 nights with several 1–2-m-class telescopes equipped with CCD (Charge-Coupled Device) cameras. As the predicted apparent magnitude of the asteroid during the period between early November and mid-December 2017 was 11–16 magnitudes, the 1–2-m-class telescopes allowed us to obtain a lightcurve with a sufficient signal-to-noise (S/N) ratio. For the sake of securing the target visibility (that is, maintaining the

Table 2. Observational circumstances.

UT date (DD/MM/YY)	RA [hr]	DEC [°]	L_{PAB} [°]	B_{PAB} [°]	α [°]	r [AU]	Δ [AU]	V [Mag]	Telescope	Seeing ["]	Sky condition
11.4/11/2017	106.44	+35.25	87.1	9.5	33.1	1.496	0.695	16.08	LOAO	3.2	Cirrus
12.4/11/2017	106.49	+35.35	87.2	9.5	32.9	1.485	0.675	15.99	LOAO	2.7	Cirrus
13.4/11/2017	106.52	+35.45	87.3	9.6	32.8	1.473	0.654	15.90	LOAO	2.7	Cirrus
16.8/11/2017	106.47	+35.86	87.6	9.6	32.1	1.432	0.583	15.57	TShAO	3.2	Clear
19.8/11/2017	106.22	+36.29	87.8	9.6	31.3	1.396	0.522	15.26	TShAO	2.5	Clear
19.9/11/2017	106.22	+36.30	87.8	9.6	31.3	1.395	0.522	15.25	MAO	2.3	Clear
20.8/11/2017	106.08	+36.45	87.9	9.6	31.1	1.384	0.503	15.15	TShAO	2.3	Clear
20.9/11/2017	106.07	+36.46	87.9	9.6	31.0	1.383	0.502	15.14	MAO	2.2	Clear
21.8/11/2017	105.91	+36.62	87.9	9.7	30.7	1.371	0.483	15.03	TShAO	2.8	Clear
21.9/11/2017	105.90	+36.63	87.9	9.7	30.7	1.370	0.482	15.02	MAO	1.8	Clear
22.8/11/2017	105.70	+36.81	87.9	9.7	30.4	1.359	0.463	14.91	TShAO	3.6	Clear
22.9/11/2017	105.69	+36.82	87.9	9.7	30.4	1.358	0.462	14.90	MAO	1.7	Clear
23.9/11/2017	105.44	+37.02	88.0	9.7	30.0	1.345	0.442	14.78	MAO	1.7	Cirrus
24.7/11/2017	105.21	+37.18	88.0	9.7	29.7	1.335	0.427	14.68	SOAO	4.8	Cirrus
26.7/11/2017	104.48	+37.65	87.9	9.8	28.8	1.309	0.389	14.40	SOAO	4.2	Clear
27.9/11/2017	103.91	+37.98	87.8	9.9	28.2	1.293	0.365	14.22	MAO	3.7	Cirrus
01.6/12/2017	101.34	+39.22	87.3	10.1	25.9	1.242	0.294	13.60	BOAO	1.7	Clear
07.6/12/2017	91.75	+42.39	84.4	11.0	20.7	1.156	0.185	12.28	CBNUO	3.5	Clear
15.2/12/2017	33.6	+40.54	64.1	14.2	41.4	1.040	0.076	10.72	OWL	4.8	Clear
15.6/12/2017	26.86	+38.13	61.1	14.3	46.6	1.033	0.073	10.76	SLT	4.2	Cirrus
16.2/12/2017	18.28	+34.17	57.1	14.3	54.1	1.023	0.070	10.86	OWL	4.3	Clear
17.1/12/2017	5.23	+26.07	50.1	13.7	67.2	1.008	0.068	11.18	OWL	4.5	Clear

Notes. *UT* date corresponding to the mid time of the observation, J2000 coordinates of Phaethon (*RA* and *DEC*), Phase Angle Bisector (PAB) - the bisected arc between the Earth-asteroid and Sun-asteroid lines - ecliptic longitude (L_{PAB}) and ecliptic latitude (B_{PAB}), the solar phase angle (α), the heliocentric (r) and the topocentric distances (Δ), the apparent predicted magnitude (V), average seeing and sky condition.

declination coordinate of Phaethon at larger than 25 degrees and performing continuous observations), observatories in the Asian and American continents located in the northern hemisphere were used. We employed the Sobaeksan Optical Astronomy Observatory (SOAO) 0.6-m, ChungBuk National University Observatory (CBNUO) 0.6-m, and Bohyunsan Optical Astronomy Observatory (BOAO) 1.8-m telescopes in Korea; the Optical Wide-field patrol (OWL) 0.5-m and Lemonsan Optical Astronomy Observatory (LOAO) 1.0-m telescopes in Arizona, USA; the Tian Shan Astronomical Observatory (TShAO) 1.0-m telescope in Kazakhstan; the Maidanak Astronomical Observatory (MAO) 0.6-m North telescope in Uzbekistan; and the Lulin Super Light Telescope (SLT) 0.4-m telescope in Taiwan. The details of the observatories, including the instruments, are shown in Table 1. Out of 22 nights of observations, all images acquired using the LOAO 1.0 m telescope were obtained in the non-sidereal tracking mode corresponding to the predicted motion of the object, whereas the other telescopes were guided at sidereal rates. During the observations made in the sidereal rate, the maximum exposure time did not exceed 200 sec. The exposure time was determined by two factors. The apparent motion of the asteroid had to be less than the nightly average full width at half maximum (FWHM) of the stellar profiles at each observatory, and the S/N ratio of the object had to be >70 .

Details of the observational circumstances are shown in Table 2. The phase angle bisector (PAB) is the bisected arc between the Earth-asteroid and Sun-asteroid lines that is expressed in ecliptic longitude (L_{PAB}) and ecliptic latitude (B_{PAB}). Observation conducted in a wide range of

PABs is essential for deriving the pole orientation and three-dimensional (3D) shape model. For this purpose, we observed Phaethon at different geometries between the Earth and the asteroid with respect to the Sun. The viewing geometry - especially during the close approaching phase - dramatically changed around UT 23:00 on 16 December 2017. The observation using the OWL 0.5-m telescope in Arizona, USA was conducted before and after the closest approach of Phaethon. The weather during each observational run was mostly clear; however, on the nights of 11–13 November 2017 at Mt. Lemmon, USA, 24 November 2017 at Mt. Sobaek, Korea, 23, 27 November in Maidanak, Uzbekistan, and 15 December 2017 in Taiwan, we observed cirrus. To characterise the rotational status of Phaethon, time-series observations were performed, mostly using the Johnson R filter, because the combinations of the R band and the optical imagers provide the highest sensitivity for rocky bodies in the solar system. In addition, observing runs dedicated to the calibration of the datasets from different telescopes were performed using the LOAO 1.0 m telescope in January 2018. To calibrate all the data obtained from various telescopes, the same CCD fields during the observing run between November and the beginning of December in 2017 were taken on a single photometric system using the LOAO 1.0-m telescope.

3. Data reduction and lightcurve analysis

All data-reduction procedures were performed using the Image Reduction and Analysis Facility (IRAF) software package. Individual images were calibrated using standard processing routine of the IRAF task *noao.imred.ccdred.ccdproc*. Bias and dark frames with relatively large standard deviations were not used for our analysis. Twilight sky flats were acquired before sunrise and after sunset and combined to produce a master flat image for each night. The instrumental magnitudes of Phaethon were obtained using the IRAF *apphot* package; the aperture radii were set to be equal to FWHM of the stellar profile on each frame in order to maximise the S/N ratio (Howell 1989). The lightcurve of Phaethon was constructed on the basis of the relative magnitude, which is the difference between the instrumental magnitude of the asteroid and the average magnitude of each comparison star. To choose a set of comparison stars, we used the dedicated photometric analysis software subsystem for asteroids, which is called the Asteroid Spin Analysis Package (see Kim 2014, for more details). This package helps to find appropriate comparison stars from single night images and to derive the spin parameters. In consequence, we selected three to five comparison stars with typical scatter of 0.01–0.02 magnitudes. The observation time (UT) was corrected for the light-travel time, and the influence of the distance from the Earth and the Sun was corrected.

To determine the periodicity of the lightcurve, the fast chi-squared (F_{χ^2}) method (Palmer 2009) was adopted. In addition, the result was confirmed via the discrete Fourier transform algorithm (Lenz & Breger 2005). These different techniques yield similar results, for example rotation periods of 3.6043 and 3.6039 h, respectively, which is consistent with previous lightcurve observations of Phaethon (Wisniewski et al. 1997; Pravec et al. 1998; Krugly et al. 2002; Ansdell et al. 2014; Warner 2015; Schmidt 2018).

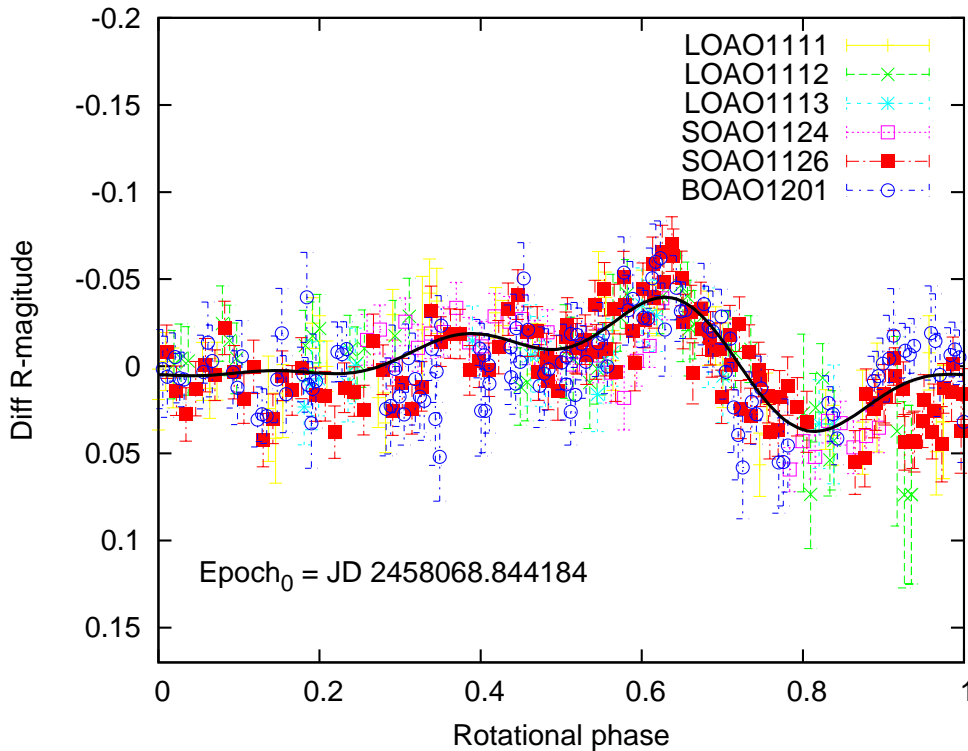


Fig. 1. Composite lightcurve of Phaethon folded with the rotational period of 3.604 h at the zero epoch of JD 2458068.844184. The black solid line is a fit to the fourth-order Fourier model using the F_{χ^2} method. Each data point represents observatories (see abbreviations in Table 1) and observing dates (MMDD).

The F_{χ^2} technique presented here employs a Fourier series truncated at the harmonic H :

$$\Phi_H(\{A_0 \dots A_H, f\}, t) = A_0 + \sum_{h=1 \dots H} A_{2h-1} \sin(h2\pi ft) + A_{2h} \cos(h2\pi ft) \quad (1)$$

We fit the fourth-order Fourier function with $A_0 = -0.00187142$, $A_1 = -0.00899222$, $A_2 = -0.0169267$, $A_3 = -0.00845652$, $A_4 = 0.00929936$, $A_5 = 0.011695$, $A_6 = -0.002285$, $A_7 = -0.00194544$, and $A_8 = -0.00699133$. We also obtained the highest spectral power at $P = 13.31869$ cycles/day using the discrete Fourier transform algorithm. As a result, a rotational period of 3.6039 h was obtained, assuming a double-peaked lightcurve. We present the resultant composite lightcurve of Phaethon in Fig. 1, which folds with the period of 3.604 h at the epoch t_0 of JD = 2458068.844184. We combined the data obtained from the SOAO, LOAO, and BOAO telescopes and computed the relative magnitudes according to the observations of comparison stars, using the observations conducted on 5–6 January 2018 as a reference for our calibration procedure.

The amplitude of the lightcurve computed via curve fitting (black solid line in Fig. 1) is $\Delta m = 0.075 \pm 0.035$. The peak-to-peak variations in magnitude are caused by the change in the apparent cross-section of the rotating tri-axial ellipsoid, with semi-axes a , b , and c , where $a > b > c$ (rotating about the c axis). According to Binzel et al. (1989), the lightcurve amplitude varies as a function

Table 3. Sidereal rotational period and pole orientation of Phaethon.

λ_1 (deg)	β_1 (deg)	λ_2 (deg)	β_2 (deg)	P_{sid} (hr)	References
308 ± 10	-52 ± 10			3.603957	This work (LI)
322 ± 10	-40 ± 10			3.603956	This work (SAGE)
319 ± 5	-39 ± 5	84 ± 5	-39 ± 5	3.603958 ± 0.000002	Hanuš et al. (2016)
		85 ± 13	-20 ± 10	3.6032 ± 0.0008	Ansdell et al. (2014)
276	-15	97	-11	3.59060	Krugly et al. (2002)

Notes. The ecliptic longitude (λ) and latitude (β) of the asteroid pole orientation, the sidereal rotational period (P_{sid}), and references. Our solutions are derived from lightcurve inversion (LI) method and shaping asteroid models using the genetic evolution (SAGE) algorithm, respectively.

of the polar aspect viewing angle θ (the angle between the rotation axis and the line of sight):

$$\Delta m = 2.5 \log\left(\frac{a}{b}\right) - 1.25 \log\left(\frac{a^2 \cos^2 \theta + c^2 \sin^2 \theta}{b^2 \cos^2 \theta + c^2 \sin^2 \theta}\right) \quad (2)$$

The lower limit of axis ratio a/b can be expressed as $a/b = 10^{0.4\Delta m}$, assuming an equatorial view ($\theta = 90^\circ$). From this calculation, the lower bound for the a/b axis ratio of Phaethon is 1.07.

4. Shape model and pole orientation

The lightcurve-inversion method (Kaasalainen & Torppa 2001; Kaasalainen et al. 2001) is a powerful tool for acquiring the rotational status, including the spin orientation and the shape of asteroids, from the disk-integrated time-series photometric data. For this purpose, the lightcurve data obtained over three or four apparitions are essential. For this reason, we utilised as many lightcurves of Phaethon as possible, mainly based on our observations but also with data available in the literature from the Database of Asteroid Models from Inversion Techniques (Durech et al. 2010) and the Asteroid Lightcurve Database (Warner et al. 2009). The detailed information and references of each lightcurve from the database are shown in Table A.1 in Appendix A. The total number of input datasets is 114 lightcurves, and the time span of the observations is 1994 to 2017. A first-period search using the *period_scan* programme was conducted between 1 and 24 h to find the global minimum χ^2 value, and the results were scanned between 3.3 and 3.9 h with an interval coefficient of 0.8, which corresponds to 2.5×10^{-5} h to refine and find the unique sidereal period. The optimal solution was found at the sidereal period of $P = 3.603957$ h (see Fig. 2), which is consistent with a previous study (Hanuš et al. 2016). Once a unique solution for the sidereal rotational periods is determined, numerous shape models with the pole orientation are applied to find the pole pair (λ, β) by scanning the entire celestial sphere. Consequently, we found the lowest χ^2 value near (308, -52) (see Fig. 3 and Table 3), which corresponds to the first pole orientation of Hanuš et al. (2016) preferred there due to a better fit to the thermal infrared data from Spitzer. There is a common practice to consider the solution as unique if there is only one pole solution that gives a significantly lower χ^2 (by 10%) than all others (Hanuš et al. 2011).

We present the 3D shape model of Phaethon based on the unique solution with a sidereal period of 3.603957 h and a pole orientation of (308, -52) (see Fig. 4). The actual value of the a/b ratio from

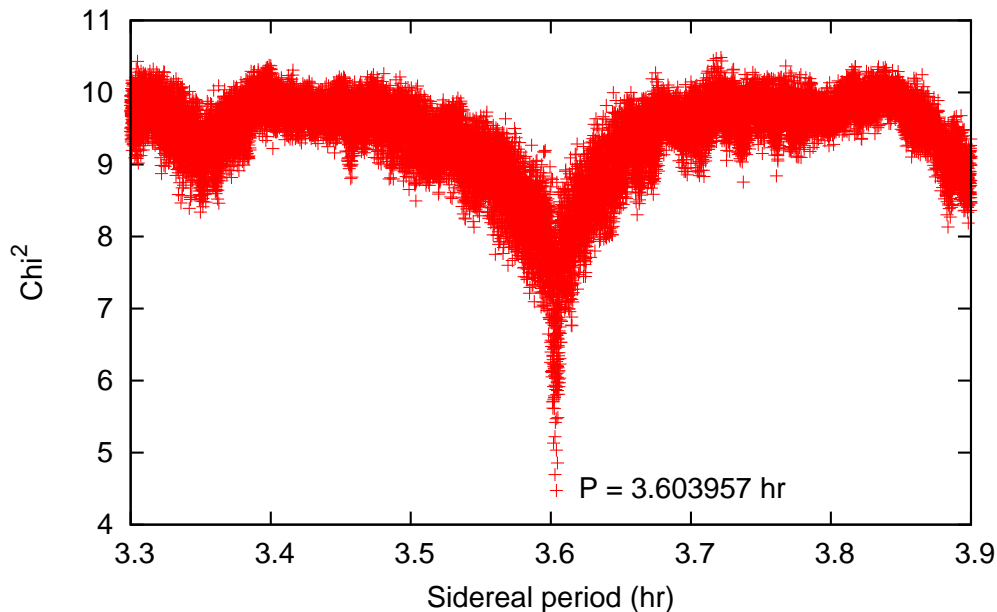


Fig. 2. Periodograms of Phaethon obtained from the period scan programme. The rotation period subspace exhibits one prominent minimum corresponding to the period of $P = 3.603957 \text{ h}$.

the 3D model solution is 1.118. So we confirm the lower bound for the a/b axis ratio obtained from the lightcurve amplitude. In addition, the spin solution was confirmed by the model from the independent SAGE method (Bartczak & Dudziński 2018). The SAGE method is based on photometric data and uses a genetic evolution algorithm to fit the model's shape and spin parameters to the lightcurves. Assuming homogeneous mass distribution, the spin axis of the resulting non-convex shape goes through the centre of mass and lies along the axis with the largest moment of inertia. The RMS (root mean square) values of the model fit from the lightcurve inversion (LI) method and SAGE algorithm are 0.02378 and 0.02738, respectively. Comparing two models from the composite lightcurves for a subset of the observation, the convex and non-convex models are generally similar to each other (see Fig. A.1). Although the SAGE model gives a better fit to explain the minima and maxima of the lightcurves in some data, for many other lightcurves the convex model fits much better than the SAGE model.

The non-convex shape model from the SAGE method is also shown in Fig. 4. The convex and non-convex models are practically not elongated in shape, which is a predictable result from the lightcurve amplitude. In comparison with the convex model, the non-convex one has some concavity features. In general, however, a non-convex model cannot be uniquely determined based on the photometric lightcurve only. Because it is possible to reconstruct the different shapes of concavities along the same line, these recesses produce a shadow effect due to one concavity of a different shape (Viikinkoski et al. 2017). Recently, a number of works for the reconstruction of a non-convex model have been conducted giving weight to various sources (i.e. adaptive optics, lightcurve, and stellar occultation) (see Hanuš et al. 2017; Viikinkoski et al. 2017, and references therein). There is one asteroid (3103 Eger) that has a non-convex model with photometry only

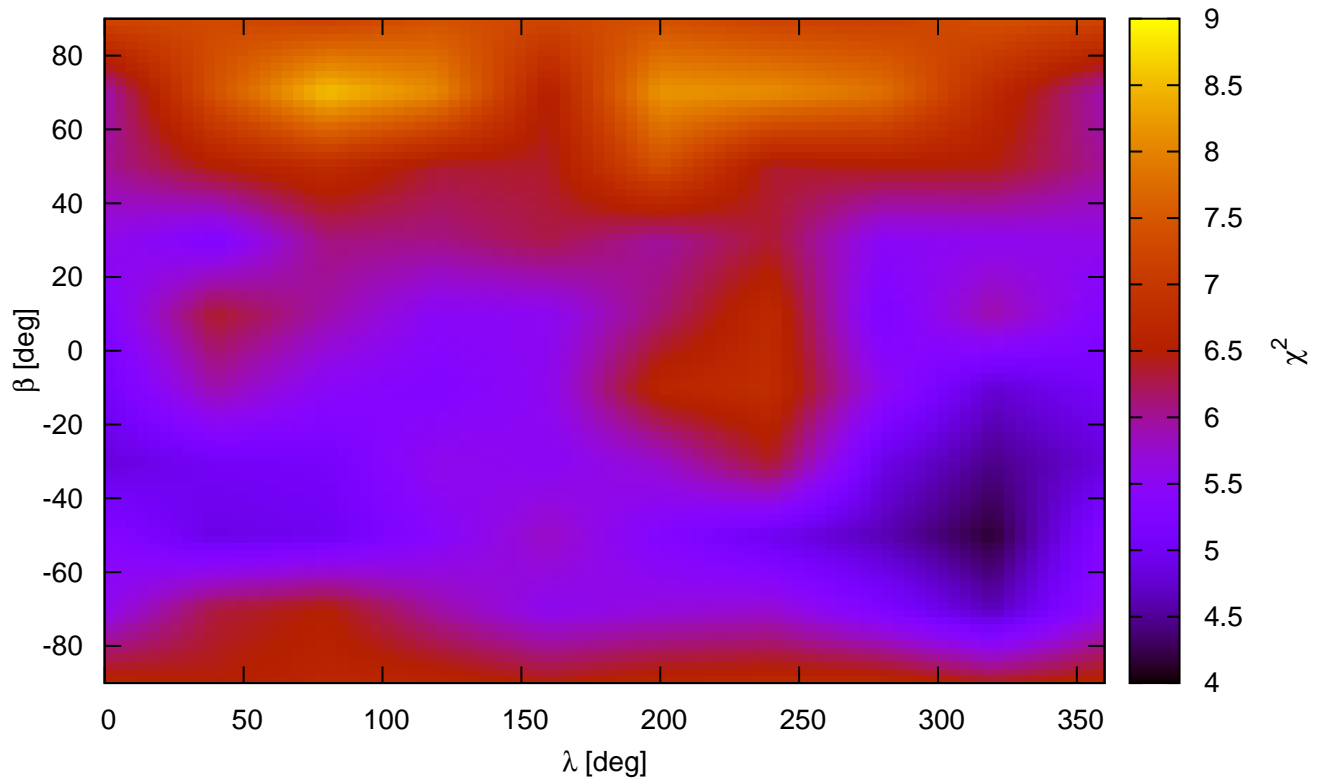


Fig. 3. Pole solution distribution of Phaethon. The lowest χ^2 value near (308, -52) was found from the lightcurve inversion method. λ and β are the ecliptic longitude and latitude of the pole orientation, respectively

(Durech et al. 2012). Its non-convex shape model better fits the lightcurves that were observed at large phase angles than a convex one.

5. Conclusions

The observation campaign for Phaethon was performed on the Asian and American continents owing to their favourable observation conditions at the end of 2017. We employed eight 1–2-m-class telescopes for a total of 22 nights between 11 November and 17 December 2017. The observation at the closest approach point on 16 December 2017 was conducted when the geometric configuration between the Earth and the asteroid with respect to the Sun changed dramatically. According to our observation datasets, we obtained the composite lightcurve of Phaethon, finding a synodic rotational period of 3.6039 ± 0.0004 h using two independent methods, and we calculated the lightcurve amplitude to be 0.095 ± 0.035 , which is regarded as a nearly spherical shape.

In addition, we derived sidereal rotational periods of 3.603957 and 3.603956 h and pole orientations of (308, -52) and (322, -40) in the ecliptic reference frame using the lightcurve-inversion method (Kaasalainen & Torppa 2001; Kaasalainen et al. 2001) and the SAGE algorithm (Bartczak & Dudziński 2018), respectively. We also obtained the 3D shape model from both methods. According to Taylor et al. (2018), there is a concavity feature near the equator from Arecibo radar observations. However, the

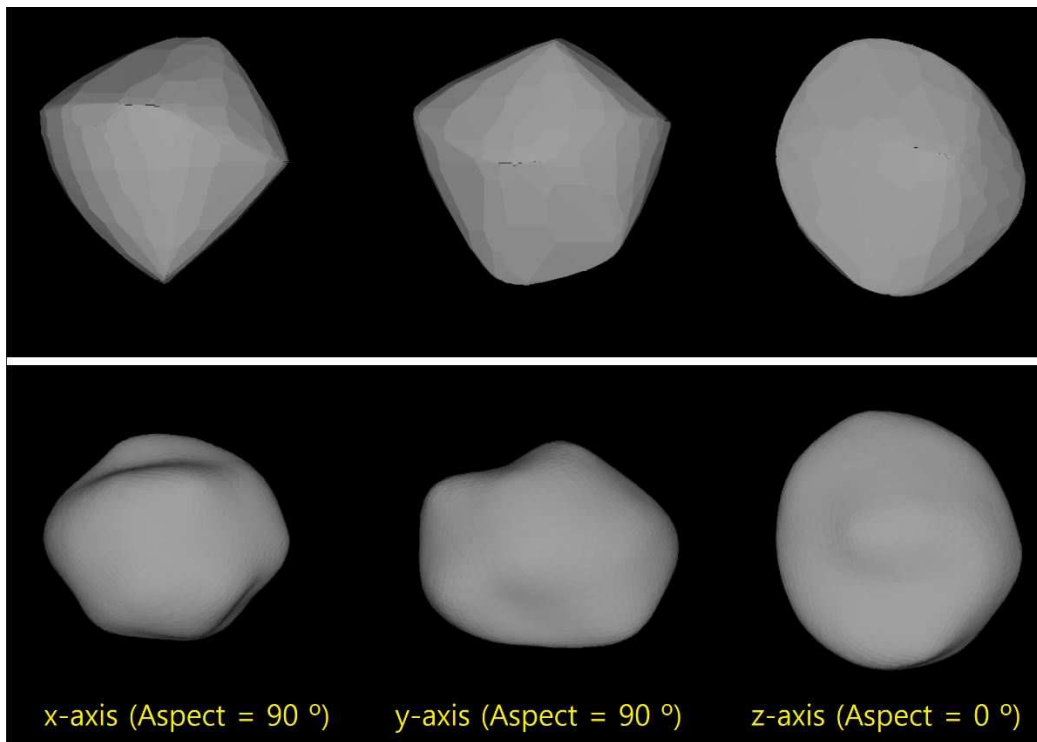


Fig. 4. Three-dimensional shape model of Phaethon obtain from LI method (top) and the SAGE algorithm (bottom). The three views in both shape models correspond to the views from the positive x, y, z axes, respectively.

features are not obviously matched with our non-convex model. Apparently, the non-convex model contains many details that may lead to misinterpretation (Durech et al. 2012). Because the RMS of the convex model is low (about 30% in chi-square), we adopt the convex model as a pole solution for Phaethon. When we examine our pole solution in the geometric configuration, the aspect angle of Phaethon was 15 deg (almost pole-on view) to 40 deg during most of the 2017 apparition, then it quickly increased to 90 deg (edge-on view) during the close approaching phase. This could well explain the fact that the lightcurve amplitude of Phaethon during the 2017 apparition is relatively smaller than other lightcurve data obtained from previous apparitions. The new shape model and pole information that were obtained here are expected to be used not only for time-resolved spectroscopic and polarimetric observation of Phaethon but also to constrain the mission design for the DESTINY⁺ science and engineering team, which is scheduled for 2022.

Acknowledgements. MJK was supported by the Korea Astronomy and Space Science Institute. The work at Adam Mickiewicz University leading to these results has received funding from the European Union’s Horizon 2020 Research and Innovation Programme, under Grant Agreement no 687378. ZYL was supported by grant number MOST 105-2112-M-008-002-MY3 and MOST 104-2112-M-259-006 from the Ministry of Science and Technology of Taiwan. AS, MK and IR were supported by the Targeted Financing Program BR05336383 Aerospace Committee of the Ministry of Defense and Aerospace Industry of the Republic of Kazakhstan.

References

- Ansdell, M., Meech, K. J., Hainaut, O., et al. 2014, *ApJ*, 793, 50
- Bartczak, P. & Dudziński, G. 2018, *MNRAS*, 473, 5050
- Binzel, R. P., Farinella, P., Zappalá, V., & Cellino, A. 1989, in *Asteroids II*, ed. R. P. Binzel, T. Gehrels, & M. S. Matthews (Tucson, AZ: Univ. Arizona Press), 416

- Binzel, R. P., Harris, A. W., Bus, S. J., & Burbine, T. H. 2001, *Icarus*, 151, 139
- Binzel, R. P., Rivkin, A. S., Stuart, J. S., et al. 2004, *Icarus*, 170, 259
- Bus, S. J. & Binzel, R. P. 2002, *Icarus*, 158, 106
- Campins, H., Hargrove, K., Pinilla-Alonso, N., et al. 2010, *Nature*, 464, 1320
- Durech, J., Sidorin, V., & Kaasalainen, M. 2010, *A&A*, 513, A46
- Durech, J., Vokrouhlický, D., Baransky, A. R., et al. 2012, *A&A*, 547, A10
- Green, S. F., Meadows, A. J., & Davies, J. K. 1985, *MNRAS*, 214, 29P
- Gustafson, B. A. S. 1989, *A&A*, 225, 533
- Hanuš, J., Delbo', M., Vokrouhlický, D., et al. 2016, *A&A*, 592, A34
- Hanuš, J., Durech, J., Brož, M., et al. 2011, *A&A*, 530, A134
- Hanuš, J., Viikinkoski, M., Marchis, F., et al. 2017, *A&A*, 601, A114
- Howell, S. B. 1989, *PASP*, 101, 616
- Jenniskens, P. 2006, *Meteor Showers and their Parent Comets* (Cambridge University Press)
- Kaasalainen, M. & Torppa, J. 2001, *Icarus*, 153, 24
- Kaasalainen, M., Torppa, J., & Muinonen, K. 2001, *Icarus*, 153, 37
- Kim, M.-J. 2014, PhD thesis, Yonsei Univ.
- Krugly, Y. N., Belskaya, I. N., Shevchenko, V. G., et al. 2002, *Icarus*, 158, 294
- Lenz, P. & Breger, M. 2005, *Communications in Asteroseismology*, 146, 53
- Palmer, D. M. 2009, *ApJ*, 695, 496
- Pravec, P., Wolf, M., & Šarounová, L. 1998, *Icarus*, 136, 124
- Rivkin, A. S. & Emery, J. P. 2010, *Nature*, 464, 1322
- Schmidt, R. E. 2018, *Minor Planet Bulletin*, 45, 131
- Taylor, P. A., Marshall, S. E., Venditti, F., et al. 2018, in *Lunar and Planetary Science Conference*, Vol. 49, Lunar and Planetary Science Conference, 2509
- Viikinkoski, M., Hanuš, J., Kaasalainen, M., Marchis, F., & Durech, J. 2017, *A&A*, 607, A117
- Warner, B. D. 2015, *Minor Planet Bulletin*, 42, 115
- Warner, B. D. 2017, *Minor Planet Bulletin*, 44, 98
- Warner, B. D. 2018, *Asteroid Lightcurve Photometry Database*
- Warner, B. D., Harris, A. W., & Pravec, P. 2009, *Icarus*, 202, 134
- Williams, I. P. & Wu, Z. 1993, *MNRAS*, 262, 231
- Wisniewski, W. Z., Michałowski, T. M., Harris, A. W., & McMillan, R. S. 1997, *Icarus*, 126, 395

Appendix A: Additional table and figures**Table A.1.** List of the lightcurve references from DAMIT and LCDB.

No	Epoch [UT]	N_p	α [°]	r [AU]	Δ [AU]	Telescopes	References
1	1994-11-02.1	22	25.5	1.82	1.04	D65	Hanuš et al. (2016)
2	1994-12-02.9	14	10.9	1.53	0.56	D65	Hanuš et al. (2016)
3	1994-12-04.1	17	11.2	1.51	0.54	D65	Hanuš et al. (2016)
4	1994-12-06.9	13	13.0	1.48	0.52	D65	Hanuš et al. (2016)
5	1994-12-27.3	76	48.0	1.22	0.44	Lowell	Ansdell et al. (2014)
6	1995-01-04.4	11	63.2	1.10	0.46	UH88	Ansdell et al. (2014)
7	1995-01-04.8	45	63.9	1.10	0.46	D65	Pravec et al. (1998)
8	1995-01-05.4	79	64.9	1.09	0.46	UH88	Ansdell et al. (2014)
9	1997-11-01.1	88	48.3	1.32	0.78	D65	Pravec et al. (1998)
10	1997-11-02.1	80	48.9	1.31	0.76	D65	Pravec et al. (1998)
11	1997-11-11.6	39	57.0	1.18	0.56	UH88	Ansdell et al. (2014)
12	1997-11-12.6	52	58.2	1.16	0.54	UH88	Ansdell et al. (2014)
13	1997-11-21.6	48	74.1	1.02	0.39	UH88	Ansdell et al. (2014)
14	1997-11-22.6	47	76.7	1.01	0.37	UH88	Ansdell et al. (2014)
15	1997-11-25.6	24	85.7	0.95	0.34	UH88	Ansdell et al. (2014)
16	1998-11-22.1	14	9.0	2.31	1.36	IAC-80	Hanuš et al. (2016)
17	1998-11-23.1	16	9.2	2.31	1.36	IAC-80	Hanuš et al. (2016)
18	1998-12-08.0	9	15.3	2.26	1.39	IAC-80	Hanuš et al. (2016)
19	1998-12-09.0	15	15.8	2.25	1.40	IAC-80	Hanuš et al. (2016)
20	2004-11-19.5	38	13.6	1.78	0.83	UH88	Ansdell et al. (2014)
21	2004-11-21.6	51	12.4	1.76	0.81	UH88	Ansdell et al. (2014)
22	2004-11-22.4	35	12.0	1.75	0.80	UH88	Ansdell et al. (2014)
23	2004-12-05.0	101	12.2	1.63	0.67	D65	Hanuš et al. (2016)
24	2004-12-05.3	41	12.4	1.63	0.67	Badlands Observatory	Hanuš et al. (2016)
25	2004-12-11.0	148	18.1	1.57	0.64	D65	Hanuš et al. (2016)
26	2004-12-18.8	15	27.9	1.48	0.61	D65	Hanuš et al. (2016)
27	2007-11-17.2	47	44.6	1.28	0.51	Modra	Hanuš et al. (2016)
28	2007-11-28.2	96	54.1	1.13	0.29	Modra	Hanuš et al. (2016)
29	2007-12-04.1	232	69.9	1.03	0.18	Modra	Hanuš et al. (2016)
30	2013-11-20.3	24	61.5	1.07	0.80	UH88	Ansdell et al. (2014)
31	2013-11-23.3	16	58.2	1.12	0.84	UH88	Ansdell et al. (2014)
32	2013-12-03.2	20	49.6	1.26	1.02	Lowell	Ansdell et al. (2014)
33	2013-12-11.3	36	44.6	1.37	1.18	UH88	Ansdell et al. (2014)

Table A.1. List of the lightcurve references from DAMIT and LCDB (cont').

N	Epoch [UT]	N_p	α [°]	r [AU]	Δ [AU]	Telescopes	References
34	2014-11-27.3	89	9.3	1.82	0.85	CS3-PDS	Warner (2015)
35	2014-11-28.2	84	9.3	1.81	0.85	CS3-PDS	Warner (2015)
36	2014-11-28.4	58	9.3	1.81	0.84	CS3-PDS	Warner (2015)
37	2014-11-29.3	82	9.4	1.80	0.84	CS3-PDS	Warner (2015)
38	2014-11-29.5	27	9.5	1.80	0.84	CS3-PDS	Warner (2015)
39	2014-12-08.0	4	14.6	1.72	0.78	CS3-PDS	Warner (2015)
40	2014-12-10.1	91	16.4	1.71	0.78	C2PU	Hanuš et al. (2016)
41	2014-12-11.9	92	18.1	1.69	0.77	C2PU	Hanuš et al. (2016)
42	2014-12-14.2	52	20.4	1.67	0.77	CS3-PDS	Warner (2015)
43	2014-12-15.3	73	21.4	1.66	0.77	CS3-PDS	Warner (2015)
44	2015-01-13.9	54	48.0	1.32	0.83	C2PU	Hanuš et al. (2016)
45	2015-01-17.9	50	50.8	1.27	0.85	C2PU	Hanuš et al. (2016)
46	2015-02-09.8	30	66.4	0.91	0.89	C2PU	Hanuš et al. (2016)
47	2015-02-10.8	41	67.2	0.89	0.89	C2PU	Hanuš et al. (2016)
48	2015-02-11.8	39	68.0	0.87	0.89	C2PU	Hanuš et al. (2016)
49	2015-08-21.6	26	27.5	2.15	2.09	UH88	Hanuš et al. (2016)
50	2015-09-08.6	22	26.6	2.24	1.90	UH88	Hanuš et al. (2016)
51	2015-09-09.6	30	26.5	2.24	1.89	UH88	Hanuš et al. (2016)
52	2015-10-08.5	21	20.0	2.33	1.60	UH88	Hanuš et al. (2016)
53	2016-11-02.2	49	33.9	1.49	0.69	CS3-PDS	Warner (2017)
54	2016-11-03.2	62	33.7	1.50	0.71	CS3-PDS	Warner (2017)
55	2016-11-04.2	119	33.5	1.51	0.72	CS3-PDS	Warner (2017)
56	2016-11-05.2	109	33.3	1.52	0.74	CS3-PDS	Warner (2017)
57	2017-11-26.3	89	29.0	1.31	0.39	CS3-PDS	Warner (2018)
58	2017-12-01.3	25	26.1	1.24	0.30	CS3-PDS	Warner (2018)
59	2017-12-01.4	24	26.0	1.24	0.29	CS3-PDS	Warner (2018)
60	2017-12-02.2	21	25.4	1.23	0.28	CS3-PDS	Warner (2018)
61	2017-12-02.3	12	25.4	1.23	0.28	CS3-PDS	Warner (2018)
62	2017-12-02.4	23	25.3	1.23	0.28	CS3-PDS	Warner (2018)
63	2017-12-17.0	424	66.8	1.01	0.06	Burleith Observatory	Schmidt (2018)

Notes. Epoch (UT date) corresponding to the mid-time of the observation, the solar phase angle (α), the heliocentric (r) and the topocentric distances (Δ). Modification of Table A.1. from Hanuš et al. (2016) to include phase angle and recent observations.

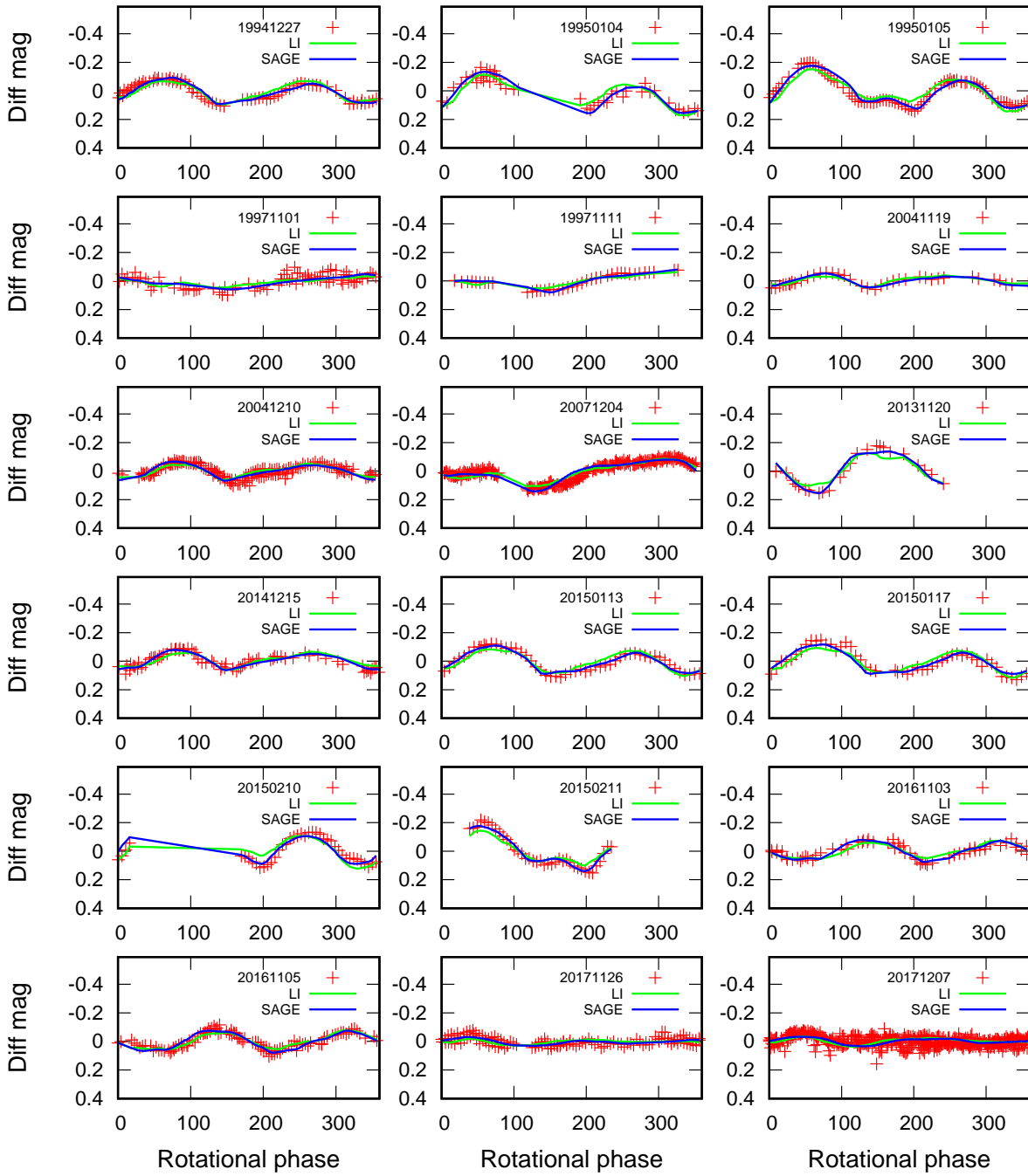


Fig. A.1. Comparison between the composite lightcurve (red cross) for a subset of the observation data (YYYYMMDD) and the model curves from the lightcurve inversion (LI) method (green fit) and SAGE algorithm (blue fit), respectively.